Comparative Biochemistry and Physiology - Part D 30 (2019) 333–346

Contents lists available at ScienceDirect

Comparative Biochemistry and Physiology - Part D

journal homepage: www.elsevier.com/locate/cbpd

This article is a part of the Special Issue on Aquaculture

Disentangling the immune response and host-pathogen interactions in Francisella noatunensis infected Atlantic cod☆

Monica Hongrø Solbakken[a], Sissel Jentoft[a,*], Trond Reitan[a], Helene Mikkelsen[b], Tone F. Gregers[c], Oddmund Bakke[d], Kjetill S. Jakobsen[a], Marit Seppola[e,*]

[a] Department of Biosciences, Centre for Ecological and Evolutionary Synthesis (CEES), University of Oslo, Oslo, Norway
[b] The Northern Norway Regional Health Authority, Tromsø, Norway
[c] Department of Biosciences, University of Oslo, Oslo, Norway
[d] Department of Biosciences, Centre for Immune Regulation, University of Oslo, Oslo, Norway
[e] Department of Medical Biology, The Arctic University of Norway, Tromsø, Norway

ARTICLE INFO

Keywords:
Atlantic cod
Francisella noatunensis
RNAseq
Immune response
Time-series
Inflammation
Host-pathogen interaction
T-cell independent B-cell activation

ABSTRACT

The genetic repertoire underlying teleost immunity has been shown to be highly variable. A rare example is Atlantic cod and its relatives Gadiformes that lacks a hallmark of vertebrate immunity: Major Histocompatibility Complex class II. No immunological studies so far have fully unraveled the functionality of this particular immune system. Through global transcriptomic profiling, we investigate the immune response and host-pathogen interaction of Atlantic cod infected with the facultative intracellular bacterium *Francisella noatunensis*. We find that Atlantic cod displays an overall classic innate immune response with inflammation, acute-phase proteins and cell recruitment through up-regulation of e.g. *IL1B*, fibrinogen, cathelicidin, hepcidin and several chemotactic cytokines such as the neutrophil attractants *CXCL1* and *CXCL8*. In terms of adaptive immunity, we observe up-regulation of interferon gamma followed by up-regulation of several *MHCI* transcripts and genes related to antigen transport and loading. Finally, we find up-regulation of immunoglobulins and down-regulation of T-cell and NK-like cell markers. Our analyses also uncover some contradictory transcriptional findings such as up-regulation of anti-inflammatory *IL10* as well as down-regulation of the NADPH oxidase complex and myeloperoxidase. This we interpret as the result of host-pathogen interactions where *F. noatunensis* modulates the immune response. In summary, our results suggest that Atlantic cod mounts a classic innate immune response as well as a neutrophil-driven response. In terms of adaptive immunity, both endogenous and exogenous antigens are being presented on MHCI and antibody production is likely enabled through direct B-cell stimulation with possible neutrophil help. Collectively, we have obtained novel insight in the orchestration of the Atlantic cod immune system and determined likely targets of *F. noatunensis* host-pathogen interactions.

1. Introduction

Atlantic cod's (*Gadus morhua* L.) unconventional immune system, compared to other teleost species, was revealed through genome sequencing showing loss of the Major Histocompatibility Complex (MHC) class II pathway, gene expansion of *MHCI* and gene losses and expansions within the family of Toll-like receptors (*TLRs*) (Star et al., 2011; Zhu et al., 2013). Although additional studies have investigated these genetic findings and hypothesized on functional outcomes (Sundaram et al., 2012; Grimholt, 2016; Malmstrom et al., 2016; Seppola et al., 2016; Solbakken et al., 2016a; Solbakken et al., 2017), no overarching transcriptional or functional examination of this particular immune system, or its interactions with pathogen, has been conducted. Furthermore, most global transcriptome studies performed on bacterial infections so far have mainly been performed in more common aquaculture or model fish species such as salmon, tilapia and zebrafish (Maekawa et al., 2019). Considering the significant amount of genetic diversity reported within the teleost immune system [examples found in references (Howe et al., 2016; Malmstrom et al., 2016; Seppola et al., 2016; Wcisel and Yoder, 2016; Zou and Secombes, 2016; Solbakken et al., 2016a; Solbakken et al., 2017; Wilson, 2017), there is a need for global approaches characterizing possible functional differences in non-model teleost species. Here, we explore the orchestration of the Atlantic cod transcriptional immune response within a host-pathogen

☆ This article is part of a special issue entitled: Aquaculture- edited by Dr. Matt Rise, Dr. Muyan Chen and Dr. Chris Martyniuk.

* Corresponding authors.
E-mail addresses: sissel.jentoft@ibv.uio.no (S. Jentoft), marit.seppola@uit.no (M. Seppola).

https://doi.org/10.1016/j.cbd.2019.04.004
Received 19 October 2018; Received in revised form 8 March 2019; Accepted 12 April 2019
Available online 13 April 2019

interaction framework using a disease affecting wild and farmed fish species worldwide: francisellosis (Birkbeck et al., 2011; Colquhoun and Duodu, 2011; Soto et al., 2013a; Leal et al., 2014; Soto et al., 2014).

In fish, francisellosis is a systemic granulomatous inflammatory disease characterized by granulomas in visceral organs such as spleen and head kidney. In Norway, it is caused by the gram-negative facultative intracellular bacterium *Francisella noatunensis* sp. *noatunensis*. Currently, there is no commercial vaccine available and treatments with antimicrobial compounds have been reported with highly variable effects (Isachsen et al., 2012; Soto et al., 2013b; Lagos et al., 2017; Ulanova et al., 2017). Initially, knowledge regarding pathogen entry, host effect and host response was derived from studies of the mammalian counterpart tularemia, which is most often caused by *F. tularensis* (Asare and Kwaik, 2010; Jones et al., 2012; Steiner et al., 2014). However, in recent years characterization of the mechanisms underlying fish-specific infections with *F. noatunensis* sp. have been conducted and demonstrate several similarities to the mechanisms described in mammals (Bakkemo et al., 2011; Birkbeck et al., 2011; Colquhoun and Duodu, 2011; Ellingsen et al., 2011; Furevik et al., 2011; Isachsen et al., 2012; Vestvik et al., 2013; Soto et al., 2013b; Brudal et al., 2014; Bakkemo et al., 2016; Klinger-Bowen et al., 2016; Lagos et al., 2017; Ulanova et al., 2017). In both fish and mammals, *Francisella* spp. resides within phagocytic cells – mainly macrophages (Bakkemo et al., 2011; Furevik et al., 2011; Vestvik et al., 2013; Brudal et al., 2014; Bakkemo et al., 2016). It likely enters through phagocytosis involving surface receptors such as mannose- and complement receptors (Asare and Kwaik, 2010; Jones et al., 2012; Steiner et al., 2014). In mammals, *Francisella* spp. are found to delay apoptosis, hampering the final stage of phagosome maturation into phagolysosomes, inhibiting the defense mechanism oxidative burst and preventing autophagy. Dysregulation of the immune response caused by *Francisella* spp. in mammals leads to excessive amounts of inflammatory cytokines and recruitment of large amounts of neutrophils. Furthermore, most of the well-described immune evasion strategies of *Francisella* spp. are shown to affect both the innate and adaptive immune system (Vojtech et al., 2009; Asare and Kwaik, 2010; Bakkemo et al., 2011; Ellingsen et al., 2011; Jones et al., 2012; Brudal et al., 2014; Steiner et al., 2014). Immune evasion is mediated through interference with interferon gamma (*IFNG*) signaling: i.e. *Francisella* spp. induces the expression of anti-inflammatory cytokines and inhibits the expression of pro-inflammatory cytokines by targeting *IFNG* receptors and preventing activation of downstream transcription factors. In mammals, *Francisella* spp. triggers the degradation of MHCII through ubiquitination restricting presentation of antigen on the cell surface, but this does not prevent a robust antibody production consisting of both immunoglobulin gamma (IgG2) and immunoglobulin mu (IgM) (Jones et al., 2012; Steiner et al., 2014). Additionally, *Francisella* spp. skews the development of the adaptive immune response towards a more tolerogenic setting, which again results in reduced activation of immune cells (Jones et al., 2012). In comparison, the effect of *F. noatunensis* on the adaptive immune system of fish is poorly characterized beyond demonstrating an increase in antibody levels that likely consists of IgM (Schrøder et al., 2009; Ellingsen et al., 2011).

Here, we characterize the overarching immune response of *F. noatunensis* infected Atlantic cod juveniles and obtain insight into the underlying host-pathogen interaction using global transcriptome profiling. Overall, Atlantic cod displays a classic acute phase response with inflammation and recruitment of immune cells. Furthermore, our results indicate that *F. noatunensis*, via host-pathogen interactions, affects innate immunity with production of anti-inflammatory cytokines, delayed apoptosis and phagosome maturation as well as inhibition of oxidative burst and autophagy. Furthermore, we also find significant changes in gene expression providing insight into the adaptive defense mechanisms of Atlantic cod indicating MHCI cross-presentation and T-cell independent B-cell activation.

Table 1
Overview of the reported number of significantly differentially expressed genes for each individual analysis.

Method	Time-point or pattern	No. of "genes"	Time-point or pattern	No. of "genes"
Trinity edgeR pairwise	6 hr up	26	6 hr down	5
	2 day up	294	2 day down	48
	4 day up	294	4 day down	179
	7 day up	134	7 day down	181
Trinity edgeR glm	6 hr up	17	6 hr down	0
	2 day up	1325	2 day down	573
	4 day up	1528	4 day down	1440
	7 day up	1187	7 day down	1532
Trinity custom	Increase	485		
	Internal max	181		
	Decrease	2688		
	Internal min	975		
	Freestyle	895		
Cufflinks pairwise	6 hr up	132	6 hr down	32
	2 day up	681	2 day down	200
	4 day up	751	4 day down	480
	7 day up	529	7 day down	601
Cufflinks custom	Increase	587		
	Internal max	395		
	Decrease	859		
	Internal min	100		
	Freestyle	351		

2. Results

In this study, we have chosen a multifaceted approach to detect differentially expressed genes. It consists of both *de novo* and reference-genome based transcriptomics (Haas et al., 2013; Trapnell et al., 2012, respectively). Collectively, we found that the different bioinformatical approaches detect similar trends (Table 1, Supplementary excel file 1), but with somewhat different sensitivities, e.g. immune-genes tend to lack predicted gene models in the genome and/or be located to poorly assembled regions (data not shown).

Overall inspection of the experiment, both by *de novo* and reference based methods, revealed good clustering of treated and control samples using MDS plots with the exception of a single sample at 6 hr post injection. The 6 hr time-point in general displays some overlap between control and treated samples (Fig. 1, Supplementary Fig. 7). Furthermore, we observe biological variation between replicates (Fig. 1, Supplementary Figs. 6 and 7), of which a large amount could be attributed to time and treatment (Fig. 1, Supplementary Figs. 3 and 4).

The different analysis approaches resulted in variable numbers of differentially expressed genes, but with similar trends (Table 1) and demonstrates the value of having high quality reference genomes and that more advanced analysis methods (e.g. generalized linear models - glm) likely results in more noise. Here, we have opted to focus on the pairwise analyses using the reference genome and then supplement with findings from the *de novo* transcriptome for specific immune genes and immune-related GO terms.

All significant differentially expressed genes from all analyses with corresponding annotation were subjected to a GO term enrichment analysis. Shortly after challenge, at 6 h, there is transcriptional up-regulation of GO term groups related to muscle function, but also terms describing immune-cell movement and inflammation as well as regulation of various cytokine production. On day 2, the GO terms describe a range of cellular responses, e.g. to biotic stimulus, various transport mechanisms, antigen presentation and cytokine production. On day 4, we observe Toll-like receptor signaling, further antigen presentation, cytokine receptor activity, and a range of regulatory activities. Finally, on day 7, the terms describe further antigen presentation, more cytokine production, and more granulocyte activity (Table 2, Supplementary excel file 2 and 3, Supplementary Figs. 13–43).

Genes reported as significantly differentially expressed and with one

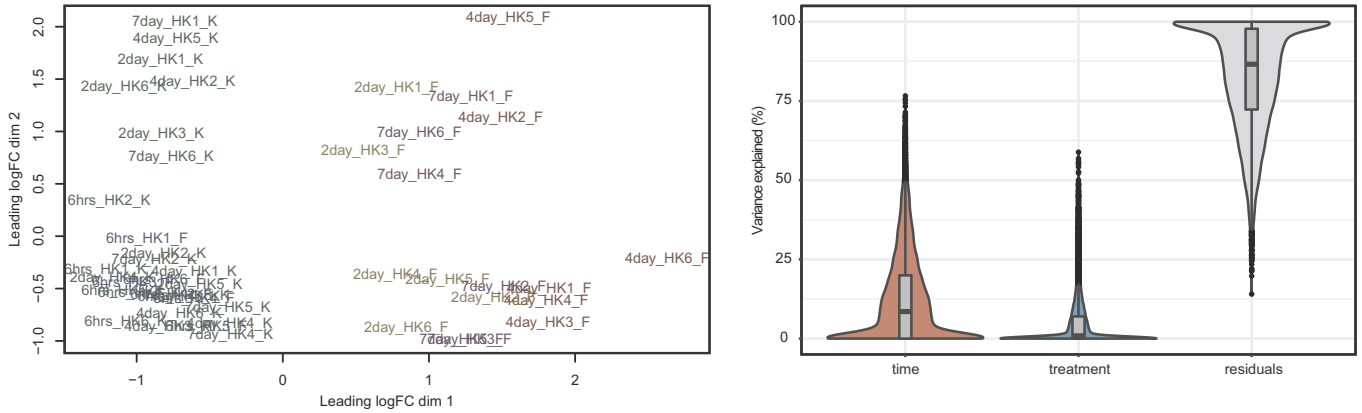

Fig. 1. MDS plot and Violin plot demonstrating the clustering of samples and variance explained by time and treatment, respectively, using counts from the *de novo* transcriptome mapping. Similar plots from the reference genome analysis are presented in Supplementary Figs. 6 and 7.

of the five predefined expression patterns (see Method section,) were also subjected to a GO term enrichment analysis. The GO terms displayed similar trends to that of the GO terms derived from the pairwise differential gene expression analyses. Genes with increasing expression levels over time indicated a response towards granulocyte macrophage colony-stimulating factor, interleukin production and lipoprotein stimulus in addition to antigen presentation. Genes with an internal maximum over time resulted in GO terms describing, among others, regulation of tumor necrosis factor production, response to lipopolysaccharide, negative regulation of apoptotic processes and response to cytokine. Genes related to wound healing (among others), were decreasing over time, whereas genes with an internal minimum (quadratic negative) expression pattern were related to a range of metabolic processes. Finally, the GO terms derived from genes with freestyle expression patterns (alternating trends over time) were related to positive regulation of ubiquitin protein transferase activity, response to unfolded protein and more (Supplementary excel file 3).

Collectively, the immune-related GO terms indicate cytokine initiation and production at 6 h, pattern recognition, antigen presentation and cell activation on day 2, further pattern recognition and antigen presentation on day 4 and 7 with increased granulocyte activity on day 7. Finally, GO terms related to acute phase responses and wound healing were related to down-regulated genes on day 7 (Fig. 2).

Looking closer at individually expressed immune genes, we observe rapid (6 h) transcriptional up-regulation of acute phase proteins fibrinogen gamma chain (*FGG*) and transferrin (*TF*), cytokines *IL1B*, *IL10*, C-C motif chemokine 1 (*CCL1*), *CCL3* and C-X-C motif chemokine 8 (*CXCL8*, alias *IL8*), one caspase (*CASP3*), some *MHCI* transcripts, a range of immunoglobulin transcripts (*IgL* and *IgH*), a B-cell marker *CD83* and a weak up-regulation of the PRR TLR23 (Table 3).

The expression of acute phase proteins reveals an up-regulation of cathelicidin antimicrobial peptide (*CAMP*), hepcidin (*HAMP*), ceruloplasmin (*CP*), coagulation factor III (*F3*), *TF*, *FGB*, *FGG* two days post injection. We also see an initial up-regulation of several PRRs (Probable ATP-dependent RNA helicase *DHX58*, Pentraxin-related protein *PTX3* and some NACHT, LRR and CARD/PYRIN domain containing *NLRC/P*) and genes related to apoptosis (apoptosis regulation *BAX*, *CASP3*, *CASP7*, *CASP6*). Additionally, up-regulation of several cytokines (i.e. *CCL2*, *CCL13*, *CXCL10*, interferon gamma (*IFNG*), and *IL12B*) accompanies with the putative B- cell marker *CD40* and T-cell marker *CD276*. Of the ~70 predicted MHCI regions in the Atlantic cod genome, 14 were found to be differentially expressed in the pairwise analysis (Supplementary Table 5). Of these, 2 were down-regulated, 11 were up-regulated and one was initially down-regulated on day 2 to become up-regulated on day 4. Further, we uncover an additional up-regulation of genes related to antigen presentation such as protein transport protein *SEC61*, antigen peptide transporters (*TAPs*), cathepsin L (*CTSL*) and L-amino oxidase (*IL4I1*) (Table 3).

Compared to day 2, on day 4 we find similar gene expression patterns (with minor differences) for the acute phase reactants, cytokines, apoptosis-related genes and genes involved in antigen presentation presented above. Additionally, at this time point we find up-regulation of some complement components and down-regulation of *IL34*. For the PRRs, the gene expression patterns on day 2 are maintained with an additional up-regulation of *TLR25*. Moreover, we observe the significant down-regulation of the T-cell marker *CD8B* (Table 3).

On day 7, there is a strong down-regulation of many acute phase reactants. A component of the inflammasome, *PYCARD* (apoptosis-associated speck-like protein containing a CARD), appears weakly up-regulated. Some traces of apoptosis remain. Otherwise, there is still a strong cytokine presence as well as antigen presentation (Table 3).

We included qPCR experiments for a selected sub-set of immune genes to improve the resolution of expression with one additional time-point and for verification of the RNAseq analysis (Fig. 3, Supplementary Figs. 9–12). Here, we observe clear up-regulation of acute phase reactants cathelicidin and hepcidin from day 1. Cytokines are readily detectable from day 2 with the exception of *IL1B* and *IL10*, which are seen from 6 h. However, all cytokine expression levels of treated individuals approaches the level of control samples by day 7. The T-cell markers *CD8A* and *CD8B* appear actively down-regulated compared to control samples, but they display overall low expression compared to the acute phase and cytokine genes. Finally, the MHCI co-receptor *B2M* display a low, but variable expression pattern down-regulated compared to control samples (Fig. 3). The qPCR expression patterns are concordant with normalized count numbers with the exception of *IL6*, *CD8* and *B2M* (Supplementary Fig. 8). *IL6* is not found significantly differentially expressed in the transcriptomics dataset. This is likely an effect driven by large individual variations present in the RNAseq data and supported by the relatively high standard error of mean (SEM) for the qPCR data (Supplementary Fig. 8). *CD8A/B* and *B2M* display slightly different expression profiles with challenged samples higher than control samples at 6 h and day 2. However, in the transcriptome dataset these expression levels are not significant with the exception of down-regulated *CD8B* on day 7 (Table 3).

As *F. noatunensis* has a facultative intracellular lifestyle dependent on phagosome maturation, we specifically looked into genes known to be involved in phagosome maturation and antigen presentation in mammals. Using the mammalian phagosome pathway map we annotated homologous genes from the pairwise reference genome analysis reported as significantly differentially expressed on day 2 and day 4. On day 2, genes related to antigen presentation were up-regulated (Fig. 4A). However, on day 4, all *MHCI* transcripts are up-regulated,

Table 2
All enriched major GO terms, listed with their GO IDs and brief description, based on significantly up- or down-regulated genes from the pairwise reference genome based analysis method. GO terms were obtained using ClueGO in Cytoscape (see Methods section). The p-value cutoff was set to 0.05 with the exception of up-regulated genes on day 2, 4 and 7 which were run with p = 0.001 and FUSION. In addition, down-regulated genes on day 7 were run with p = 0.01. All GO term lists and networks are available in supplementary excel file 3 Gene ontology enrichment data and supplementary information. GO term IDs assigned with * have had their descriptions shortened to fit the table.

GOID	GOTerm	GOID	GOTerm
6 hr up		**4 day up cont.**	
GO:0003009	Skeletal muscle contraction	GO:0045088	Regulation of innate immune response
GO:0014909	Smooth muscle cell migration	GO:0045807	Positive regulation of endocytosis
GO:0030049	Muscle filament sliding	GO:0048583	Regulation of response to stimulus
GO:0032088*	Negative regulation of NF-kappaB	GO:0048585	Negative regulation of response to stimulus
GO:0032370	Positive regulation of lipid transport	GO:0051121	Hepoxilin metabolic process
GO:0032612	Interleukin-1 production	GO:0051246	Regulation of protein metabolic process
GO:0032649*	Regulation of IFNg production	GO:0051726	Regulation of cell cycle
GO:0032743*	Positive regulation of IL2 production	GO:0055076	Transition metal ion homeostasis
GO:0071621	Granulocyte chemotaxis	GO:0070062	Extracellular exosome
GO:0071622	Regulation of granulocyte chemotaxis	GO:0070427*	NOD domain containing 1 signaling pathway
6 hr down		GO:0071216	Cellular response to biotic stimulus
	No significant GO terms	GO:0071310	Cellular response to organic substance
2 day up		GO:1901700	Response to oxygen-containing compound
GO:0002544	Chronic inflammatory response	GO:2000352*	Negative regulation of apoptotic process
GO:0005925	Focal adhesion	**4 day down**	
GO:0006826	Iron ion transport	GO:0006094	Gluconeogenesis
GO:0015031	Protein transport	GO:0009986	Cell surface
GO:0032496	Response to lipopolysaccharide	GO:0010721	Negative regulation of cell development
GO:0034097	Response to cytokine	GO:0015081*	Na + transmembrane transporter activity
GO:0034976*	Response to ER stress	GO:0016208	AMP binding
GO:0042254	Ribosome biogenesis	GO:0019062	Virion attachment to host cell
GO:0042470	Melanosome	GO:0020037	Heme binding
GO:0042590*	Exogenous antigen presentation, MHCI	GO:0033198	Response to ATP
GO:0045807	Positive regulation of endocytosis	GO:0033293	Monocarboxylic acid binding
GO:0050663	Cytokine secretion	GO:0044236	Multicellular organismal metabolic process
GO:0051050	Positive regulation of transport	GO:0044283	Small molecule biosynthetic process
GO:0051121	Hepoxilin metabolic process	GO:0045837	Negative regulation of membrane potential
GO:0070062	Extracellular exosome	GO:0046530	Photoreceptor cell differentiation
GO:0070427*	NOD domain containing 1 signaling pathway	GO:0048029	Monosaccharide binding
GO:0071216	Cellular response to biotic stimulus	GO:0060219*	Eye photoreceptor cell differentiation
GO:0071222	Cellular response to lipopolysaccharide	GO:1902936	Phosphatidylinositol bisphosphate binding
GO:0071346	Cellular response to interferon-gamma	**7 day up**	
2 day down		GO:0002474*	Antigen presentation, MHCI
GO:0001738	Morphogenesis of a polarized epithelium	GO:0002479*	Exogenous antigen presentation, MHCI + TAP
GO:0007045	Cell-substrate adherens junction assembly	GO:0006986	Response to unfolded protein
GO:0016208	AMP binding	GO:0016469*	H+ transporting two-sector ATPase complex
GO:0016528	Sarcoplasm	GO:0034103	Regulation of tissue remodeling
GO:0019433	Triglyceride catabolic process	GO:0042470	Melanosome
GO:0030104	Water homeostasis	GO:0050715	Positive regulation of cytokine secretion
GO:0033293	Monocarboxylic acid binding	GO:0070062	Extracellular exosome
GO:0060343	Trabecula formation	GO:0071621	Granulocyte chemotaxis
4 day up		GO:0097530	Granulocyte migration
GO:0002224	Toll-like receptor signaling pathway	**7 day down**	
GO:0002474*	Antigen presentation, MHCI	GO:0001775	Cell activation
GO:0002544	Chronic inflammatory response	GO:0002703	Regulation of leukocyte mediated immunity
GO:0002682	Regulation of immune system process	GO:0005615	Extracellular space
GO:0004896	Cytokine receptor activity	GO:0006897	Endocytosis
GO:0005102	Receptor binding	GO:0006953	Acute-phase response
GO:0005615	Extracellular space	GO:0007200*	PLC-activating GPCR signaling pathway
GO:0005925	Focal adhesion	GO:0009986	Cell surface
GO:0006986	Response to unfolded protein	GO:0010043	Response to zinc ion
GO:0009991	Response to extracellular stimulus	GO:0010524*	Pos. regulation of Ca^{2+} transport into cytosol
GO:0010033	Response to organic substance	GO:0016051	Carbohydrate biosynthetic process
GO:0016192	Vesicle-mediated transport	GO:0019838	Growth factor binding
GO:0019838	Growth factor binding	GO:0031226	Intrinsic component of plasma membrane
GO:0019899	Enzyme binding	GO:0033293	Monocarboxylic acid binding
GO:0030198	Extracellular matrix organization	GO:0040012	Regulation of locomotion
GO:0031347	Regulation of defense response	GO:0044275	Cellular carbohydrate catabolic process
GO:0031410	Cytoplasmic vesicle	GO:0045597	Positive regulation of cell differentiation
GO:0033993	Response to lipid	GO:0046503	Glycerolipid catabolic process
GO:0042127	Regulation of cell proliferation	GO:0046718	Viral entry into host cell
GO:0042470	Melanosome		

RAB7 and tubulins (*TUBB*) are added, several integrins become up-regulated together with the fish-specific PRR *TLR25*. Furthermore, myeloperoxidase (*MPO*) and a component of the NADPH oxidase complex are down-regulated (Fig. 4B).

3. Discussion

From a mammalian point of view, a classical immune response would consist of pattern recognition, acute phase response and

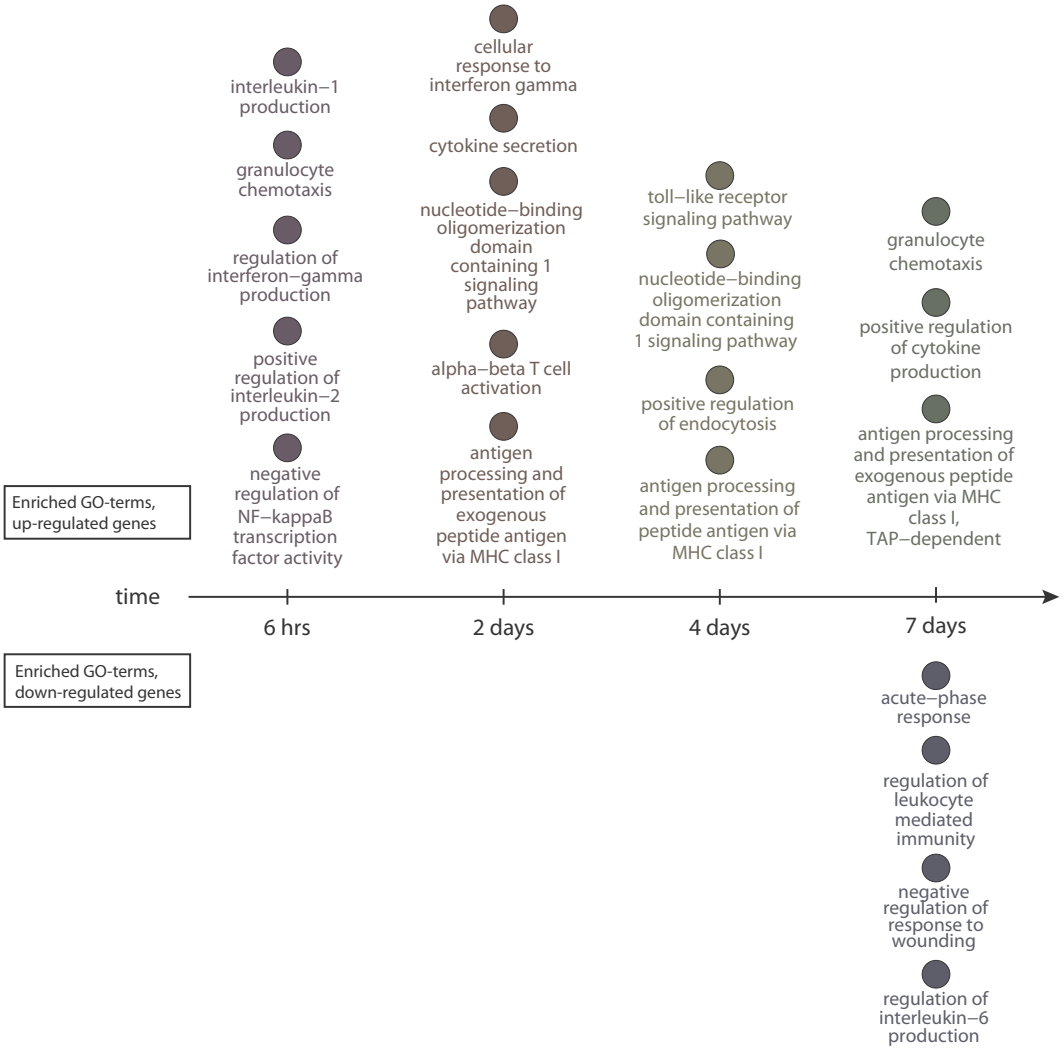

Fig. 2. Overview of the main immune-related GO terms reported as enriched from all analyses. GO terms above the time-line are derived from significantly up-regulated genes. Similarly, the GO terms below are derived from down-regulated genes. All full GO term networks are available in the supplementary information.

inflammation, antigen presentation, and finally cellular and humoral responses throughout (Zhu et al., 2013; Riera Romo et al., 2016; Wilson, 2017; Flajnik, 2018). However, the framework of this study is a non-model teleost shown to have lost the MHCII pathway. Furthermore, the pathogen has a facultative intracellular lifestyle resulting in host-pathogen interactions modulating the immune response. By using global transcriptome profiling, we here we present a more systemic overview of both the innate and adaptive immune response in Atlantic cod.

3.1. Pattern recognition by PRRs

An intracellular bacterium has to avoid detection by pattern recognition receptors (PRRs) upon host entry as well as after gaining entry into a host cell. For the host, the ability to detect a pathogen plays an important role for the overall orchestration and outcome of the immune response, and it has several different PRR families located throughout the cell responding to a range of pathogen-associated and damage-associated molecular patterns (PAMPs and DAMPs, respectively) (Kawasaki and Kawai, 2014; Brubaker et al., 2015; Drickamer and Taylor, 2015; Riera Romo et al., 2016; Wcisel and Yoder, 2016). *Francisella* spp. in mammals in known to change the properties of its surface molecules which otherwise would be recognizable PAMPs to the host. If successful, *Francisella* spp. exploits cell surface receptors to gain entry into the host immune cell (Bakkemo et al., 2011; Jones et al., 2012). Within the phagosome, and later in the cytosol, one could expect pathogen detection by intracellular PRRs. However, studies have suggested that *Francisella* spp. actively modulates the expression of intracellular PRRs to facilitate its intracellular lifestyle (Jones et al., 2012). Within this experiment, we observed differential expression of several PRR families. The most prominently up-regulated was Toll-like receptor 25 (*TLR25*), a homolog to *TLR1/2/6* in mammals (Solbakken et al., 2016b). It is putatively located to the plasma membrane, and even though there are some evidence for TLRs residing in phagosomes (Pauwels et al., 2017), it likely indicates that TLR25 detects *F. noatunensis* residing in the extracellular environment. There is also a weak up-regulation of *TLR23* at 6 h, which at later stages was found down-regulated together with *TLR22* – where both have a putatively intracellular location (Solbakken et al., 2016b). The pentraxin *PTX3* is the second most strongly expressed gene. It is a secreted PRR that facilitates pathogen recognition by dendritic cells and macrophages as well as pathogen removal by complement (Bottazzi et al., 2016). Finally, we observed a range of expressed nucleotide-binding domain and leucine-rich repeat containing (NACHT, LRR and CARD/PYRIN containing, NLRs) receptors. They reside in the cytoplasm and have both PRR and non-immune related functions related to development, tissue homeostasis and apoptosis (Kufer and Sansonetti, 2011; Howe et al., 2016). Atlantic cod has a larger repertoire of *NLRs* compared to many other

Table 3
Overview of some key immune-related genes. All logFC data is derived from the Cufflinks pairwise analysis unless otherwise stated. Genes may have significant differential expression in other analyses as well. LogFC values are separated by/according to the time-point column. * indicates that a gene has several annotated transcripts - their expression patterns are indicated in the logFC columns. ** indicates that for certain time-points a gene has several transcripts. An average logFC is depicted in the logFC for these cases For more details see Supplementary Tables 4–7 and supplementary excel file 1. ◊ Please note that NLR annotation is not fish-specific. See Howe et al. (2016) for fish-specific NLR annotations.

Overall function	Gene name	logFC	Analysis	Time-point
Acute phase protein	APCS	−1.4	Genome	Day 7
Acute phase protein, antimicrobial	CAMP	3.4	Genome	Day 2, 7
Acute phase protein, iron homeostasis	CP	2.2	Genome	Day 2
Acute phase protein	CRP	−2.0	Genome	Day 4
Acute phase protein, iron homeostasis	F3	3.7	Transcriptome	Day 2
Acute phase protein, iron homeostasis	FGA	−4.3	Genome	Day 7
Acute phase protein, iron homeostasis	FGB	1.6/2.8/−2.7	Genome	Day 2, 4, 7
Acute phase protein, iron homeostasis	FGG	6.2/3.4/−9.0	Genome	6 h, day 2, 7
Acute phase protein, iron homeostasis	FTH1	−1.6	Genome	Day 4
Acute phase protein, antimicrobial, iron homeostasis	HAMP	4.1/3.1/2.2	Genome	Day 2, 4, 7
Acute phase protein, iron homeostasis	HPX	−11.3	Transcriptome	Day 7
Acute phase protein, antimicrobial	LYGF1*	Up-regulated	Genome	Day 2, 4, 7
Acute phase protein	SERPINE1	2.4	Genome	Day 4
Acute phase protein, iron homeostasis	TF	2.0/5.4/6.0	Genome	6 h, day 2, 4
PRR	PTX3	4.0/6.4	Transcriptome	Day 2, 4
PRR	TLR22	−2.5/−3.2	Genome	Day 2, 7
PRR	TLR23	1.0/−1.2/−1.9	Genome	6 h, 4, 7
PRR	TLR25	4.4	Genome	Day 4
PRR, possible inflammasome sensor	NLRC3*◊	Variable	Genome	6 h, day 2, 4, 7
PRR, possible inflammasome sensor	NLRP12*◊	Variable	Genome	Day 2, 4
Inflammation, inflammasome component	CASP1**	1.7/1.2/2.2**	Genome	Day 2, 4, 7**
Inflammation, inflammasome component	IL1B	6.8/8.3/7.0/5.5	Genome	6 h, day 2, 4, 7
Inflammation, inflammasome component	PYCARD	1.0	Genome	Day 7
Chemoattractant	CCL1	2.2/6.0	Transcriptome	6 h, day 2
Chemoattractant	CCL13	5.8/5.9/4.7	Transcriptome	Day 2, 4, 7
Chemoattractant	CCL2	1.1/1.9/1.4	Genome	Day 2, 4, 7
Chemoattractant	CCL3*	Up-regulated	Transcriptome	6 h, day 2, 4
Chemoattractant	CXCL1	2.1	Genome	Day 4
Chemoattractant	CXCL10	3.2/3.5	Transcriptome	Day 2, 4
Chemoattractant	CXCL8*	Up-regulated	Genome	6 h, day 2, 4, 7
Cytokines, chemokines	IFNg	4.4/4.1/2.7	Transcriptome	Day 2, 4, 7
Cytokines, chemokines	IL10	5.1/6.3/4.9/4.2	Transcriptome	6 h, day 2, 4, 7
Cytokines, chemokines	IL12B	2.4/2.6	Genome	Day 2, 4
Cytokines, chemokines	IL34	−2.6/−2.9	Genome	Day 4, 7
Complement	C3	3.0	Genome	Day 4
Complement	C7	2.0	Genome	Day 4
Apoptosis	BAX	1.2/1.6	Genome	Day 2, 7
Apoptosis	CASP3	2.6/2.6/2.5	Genome	6 h, day 2, 4
Apoptosis	CASP6**	1.1/−1.4/0.9**	Genome	Day 2, 4, 7**
Apoptosis	CASP7	0.9/1.1/1.1	Genome	Day 2, 4, 7
Antigen presentation, lysosomal degradation	CTSL	3.6/3.6/3.6	Transcriptome	Day 2, 4, 7
Antigen presentation	MHCI	Variable	Genome	6 h, day 2, 4, 7
Antigen presentation, lysosomal degradation, antimicrobial	IL4I1*	Up-regulated	Transcriptome	Day 2, 4, 7
Antigen presentation	SEC61*	Up-regulated	Genome	Day 2, 4
Antigen presentation	TAP1	1.5/1.8/1	Genome	Day 2, 4, 7
Antigen presentation	TAP2	2/2.2/2.6	Transcriptome	Day 2, 4, 7
Antigen presentation	TAPBPL	1.6/1.5	Genome	Day 2, 4
B-cells	CD22*	Down-regulated	Genome	Day 2, 4
B-cells	CD40	1.3	Genome	Day 2
B-cells	CD79B	−1.2/−1.8	Genome	Day 4, 7
B-cells	CD83	1.4/3.1/2.7/1.5	Genome	6 h, day2, 4, 7
T-cells	CD276	1.2/1.6	Genome	Day 2, 4
T-cells	CD8B	−1.3/−1.7	Genome	Day 4, 7
Antibodies, heavy and light chains	IgH/IgL*	Up-regulated	Genome	6 h, day 2
Antibodies, heavy and light chains	IgH/IgL*	Down-regulated	Genome	Day 4, 7

teleosts (Torresen et al., 2018) and we observe significant differential expression from 19 unique *NLR* regions (Supplementary Table 7). Of these, a few are up-regulated in response to *F. noatunensis*, whereas most are significantly down-regulated throughout suggesting sub-functionalization of NLRs in Atlantic cod similarly to NLRs in other vertebrates (Kufer and Sansonetti, 2011). Overall, *F. noatunensis* appears to be readily detected by extracellular and surface located PRRs in Atlantic cod. However, we find no signs of detection by intracellular PRRs indicating that upon host cell entry *F. noatunensis* efficiently avoids detection.

3.2. Antimicrobials and acute phase responses

Antimicrobial peptides are found in mucus, plasma and within the extracellular space (Riera Romo et al., 2016). We find up-regulation of *HAMP* (*hepcidin*), *CAMP* (*cathelicidin*) and *LYGF1* (*alias LYG1, lysozyme g-type*), which all have antimicrobial effects (Table 3, Fig. 3, qPCR of *LYGF1* has been published earlier (Seppola et al., 2016)). The effect of antimicrobial acute phase proteins in *Francisella* spp. infections can be debated as studies demonstrate that *Francisella* spp. e.g. is able to change its cell surface charge counteracting cationic antimicrobial peptides (Jones et al., 2012). Furthermore, its facultative intracellular

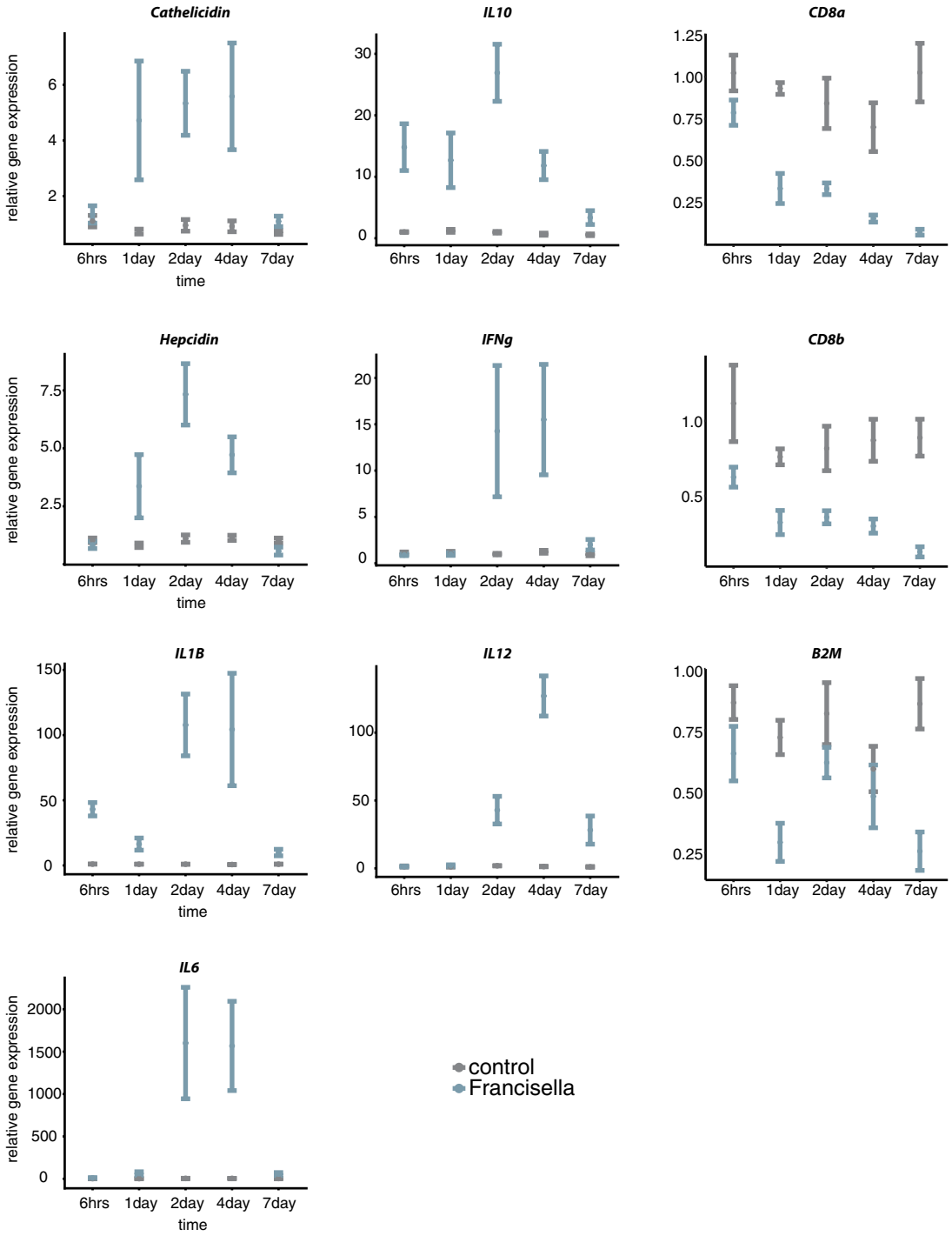

Fig. 3. Real-time qPCR data of selected immune genes. Genes are displayed with relative expression calculated in contrast to housekeeping genes (see Methods section). Please note that y-axis scales are dissimilar. Control samples are noted in grey. Challenged samples are noted in teal.

lifestyle efficiently protects it from host defenses present in the extracellular space.

Similar to the antimicrobial peptides, the acute phase proteins are also found in mucus, plasma and tissues and are made in response to inflammation. These proteins have various subfunctions related to iron homeostasis, wound healing and pattern recognition (Riera Romo et al., 2016). We observe strong up-regulation of some fibrinogen chains. Fibrinogen is involved in the coagulation cascade, but is also known to activate and modulate inflammatory processes (Riera Romo et al., 2016). We further observe up-regulation of genes involved in iron homeostasis: *FTH1* (*ferritin*), *CP* (*ceruloplasmin*), *TF* (*transferrin*), *F3* (*coagulation factor III*) and *HAMP* (*hepcidin*) (Table 3). In terms of iron, it is a key nutrient for both the host and for the pathogen. The presence of iron homeostasis related acute phase proteins is thought to sequester iron from the pool available to pathogens during infection (Nairz et al., 2018). However, in the case of intracellular pathogens, this protective mechanism could end up providing an iron source as much of the sequestered iron is moved intro e.g. macrophages (Jones et al., 2012). Overall, Atlantic cod appears to mount a relatively classic acute phase response towards *F. noatunensis*.

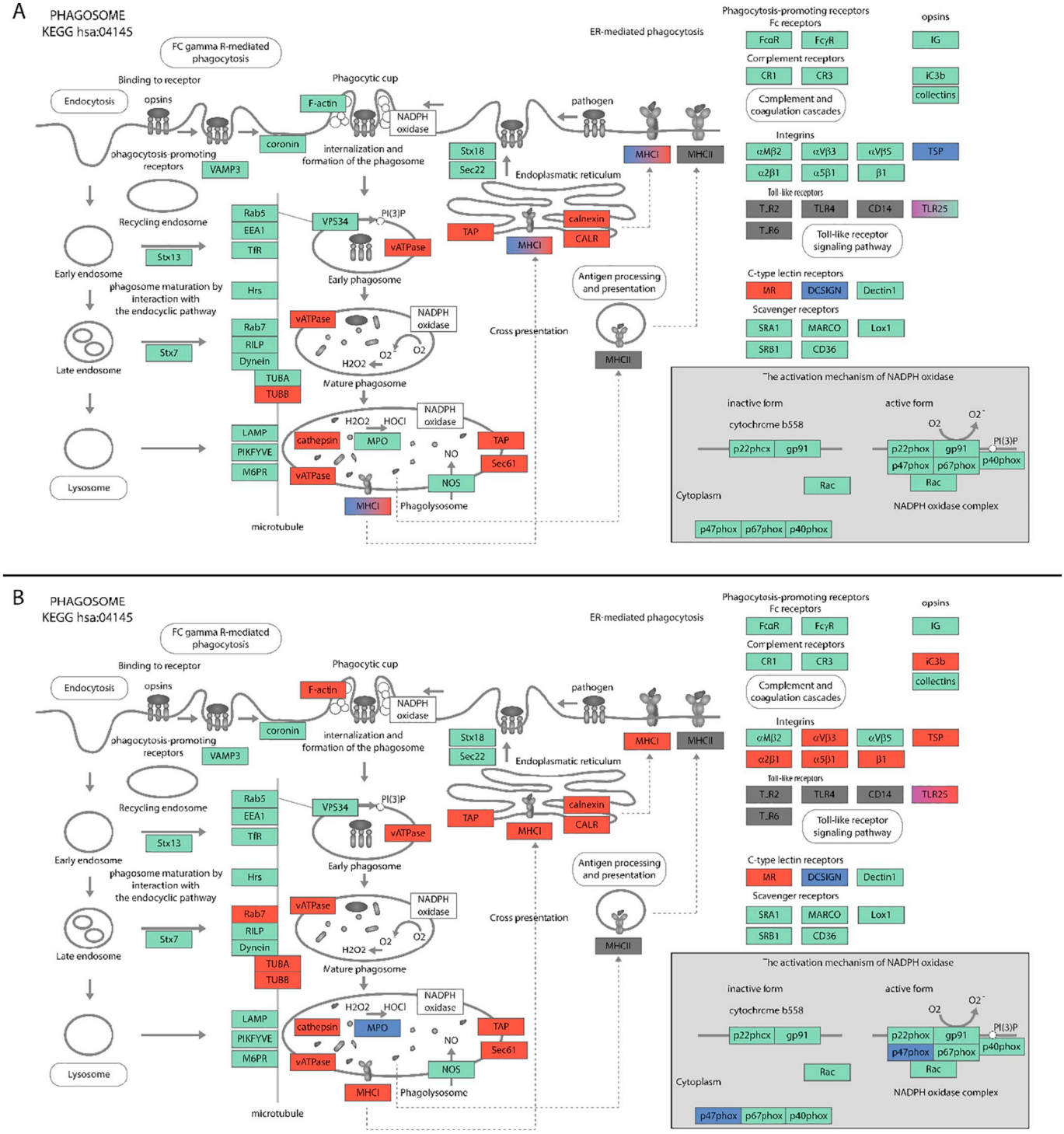

Fig. 4. The mammalian phagosome pathway displayed with significantly differentially expressed Atlantic cod homologous genes derived from the reference genome based analysis on day 2 (A) and day 4 (B), respectively. Grey genes are known to be lost from the Atlantic cod genome. Red genes are significantly up-regulated. Blue genes are significantly down-regulated. Green genes are not significantly differentially expressed (or missing annotation). The purple fish-specific TLR25 genes is proposed to be located to the plasma membrane (Solbakken et al., 2016b). MHCI on day 2 is colored with a gradient due to both up-regulated and down-regulated MHCI transcripts. The figure is drawn after the pathway map available at KEGG.

3.3. Inflammation and cytokine expression

Inflammation is the overall initial response of the innate immune system upon infection or tissue damage (Riera Romo et al., 2016). In our dataset, we observe early up-regulation of the pro-inflammatory cytokine *IL1B*. IL1B is produced after activation of pattern recognition receptors and regulates the immune response by attracting phagocytes/leukocytes and inducing expression of other cytokines (Zou and Secombes, 2016). Key to IL1B function in mammals, and central to inflammation in fish, is the inflammasome (Jones et al., 2012; Kuri et al., 2017; J.Y. Li et al., 2018; Y. Li et al., 2018). In our data *IL1B* is up-regulated from the first time-point, but the remaining components of the inflammasome (*CASP1*, *NLR*, *PYCARD*) appear gradually throughout the experiment with *PYCARD* last on day 7 (Table 3). We

also observe the up-regulation of an anti-inflammatory cytokine, *IL10*. In mammals, IL10 has been shown to suppress inflammation by down-regulating tumor necrosis factor alpha (TNF), interferon gamma (IFNG), C-X-C motif chemokine 8 (CXCL8, alias IL8), components of the NADPH oxidase complex as well as genes involved in antigen presentation (Zou and Secombes, 2011). Furthermore, studies have demonstrated that *Francisella* spp. suppresses pro-inflammatory cytokines and increases anti-inflammatory cytokines to dampen cell-mediated immune responses (Jones et al., 2012). *In vitro* studies in Atlantic cod also demonstrate up-regulation of both *IL1B* and *IL10* upon exposure to *F. noatunensis* (Bakkemo et al., 2011). As *in vivo* studies in Atlantic cod demonstrate the formation of inflammatory and granular foci in visceral organs (Gjessing et al., 2011), the presence of anti-inflammatory signals likely does not completely hinder inflammation and inflammasome assembly. Thus, our data indicate a subdued inflammatory response towards *F. noatunensis*.

We also observe up-regulation of *IL12B* (Table 3) and one chain of the IL12 receptor (IL12RB2, Supplementary excel file 1). IL12B, belonging to the IL12 family, form heterodimers with several members of its family and the functional outcome varies (Secombes, 2016). In fish species with CD4, IL12 and IFNG work together to enable differentiation of CD4+ T-cells into Th1 cells (Wang and Secombes, 2013). IL23, in combination with IL1B and TGFb will trigger differentiation of CD4+ T-cells into Th17 cells (Wang and Secombes, 2013). As Atlantic cod lacks CD4 (Star et al., 2011), other effects of IL12/IL23 such as inducing IFNG production from macrophages or stimulate blood lymphocytes may be the functional outcome (Wang and Secombes, 2013; Zou and Secombes, 2016).

There were several chemotactic cytokines up-regulated within in our experiment. There appears to be trafficking of T-cells dependent on C-C motif chemokine 1 (*CCL1*), *CCL13* and *CXCL10*, and some trafficking of NK-like cells based on *CXCL10*. *CCL3* attracts macrophages and NK-like cells (Sokol and Luster, 2015). Neutrophils appear to have the strongest presence supported by the up-regulation of *CXCL8*, a neutrophil attractant that in Atlantic cod exists in 8 copies (Havixbeck and Barreda, 2015; Solbakken et al., 2016b). This is further supported by another neutrophil attractant *CXCL1* (Sokol and Luster, 2015). Lastly, there is positive enrichment of hepoxilin-metabolism related genes (Table 2, Supplementary excel file 2). A suggested function for these genes has been in inflammation and recruitment of neutrophils across endothelial cell layers in mammals in addition to their involvement in fatty acid metabolism (Szabady and McCormick, 2013). Collectively, these transcripts indicate that Atlantic cod commits a neutrophil-driven defense upon infection with *F. noatunensis*.

The final cytokine up-regulated is interferon gamma (*IFNG*) - key regulator in the transition from innate to adaptive immunity. It is an important activator of monocytes/macrophages, facilitates pathogen clearance by increased nitric oxide production and phagocyte activity, induces autophagy, stimulates T-cells and increases antigen presentation on MHCI and MHCII (Jones et al., 2012; Wiegertjes et al., 2016; Zou and Secombes, 2016). Cells treated with IFNG usually respond with increased expression of genes related to inflammation such as TNF, IL34 and iNOS (NOS2) and other immune-related genes like ubiquitin-like protein ISG15 and components of the NADPH oxidase complex. We observe an *IFNG* response on day 2 and 4. Similarly, we observe up-regulation of *ISG15* on day 2 (Supplementary excel file 1). However, we observe down-regulation of *IL34* and observe no differential expression of *TNF* or *NOS2* (Supplementary excel file 1). *Francisella* spp. is known to inhibit the IFNG signaling pathway by down-regulating its receptor IFNGR1 and the required IFNGR1 transcription factor STAT1. Simultaneously, it will increase the expression of SOCS3 - an inhibitor of IFNG signaling (Jones et al., 2012). We find up-regulation of *SOCS3* on day 2 and day 4. In contrast, we observe up-regulation of STAT1 and no significant differential expression of IFNGR1 (Supplementary excel file 1). Thus, the transcriptional *IFNG* response in this study appears to be modulated by *F. noatunensis*.

3.4. Phagosome maturation and antigen presentation

As *Francisella* spp. infect and replicate within phagocytic cells like macrophages and neutrophils, it has evolved evasion mechanisms preventing their clearance. One of these mechanisms is the delay of phagosome maturation, inhibiting the production of reactive oxygen and nitrogen species with subsequent oxidative burst aimed at clearing phagocytosed material and prevention of autophagy (McCaffrey and Allen, 2006; Asare and Kwaik, 2010; McCaffrey et al., 2010; Jones et al., 2012; Steiner et al., 2014). Functionally, this inhibitory effect has also been observed in Atlantic cod (Vestvik et al., 2013). Here, we find evidence of an active phagosome pathway, seemingly increasing in activity over time in terms of antigen presentation (Fig. 4). However, we found an overall down-regulation of neutrophil cytosolic factor 1 (*NCF1* alias *p47phox*), a part of the NADPH activating complex enabling production of reactive oxygen species. This complex should be up-regulated as a response towards the increased expression of *IFNG* in our study, but is likely down-regulated due to *IL10* (Zou and Secombes, 2016). Furthermore, the degrading environment within the phagosome is dependent on MPO (Klebanoff et al., 2013), which we also find down-regulation in our study (Table 3, Fig. 4, Supplementary excel file 1). In conclusion, the transcriptional patterns observed here indicate a Francisella-friendly phagosome environment.

Throughout the experiment, we observed enrichment of antigen presentation pathways (Tables 2 and 3). *MHCI* expression is affected by both IFNG and IL10, both up-regulated in our study, positively and negatively, respectively (Zou and Secombes, 2016). Atlantic cod has a large expansion of *MHCI* (Star et al., 2011) and we found 14 *MHCI* regions in the genome with reported significant differential expression in the pairwise analysis. Of these, the majority were up-regulated (Supplementary Table 5) indicating a stronger effect from IFNG than IL10. Connected to *MHCI*, we observed overall expression of genes related to antigen presentation (protein transport protein *SEC61*, antigen peptide transporters (*TAPs*), cathepsin L (*CTSL*) and L-amino oxidase (*IL4I1*)) as well as several proteasomal subunits and ubiquitin ligases (Table 3, Supplementary excel file 1). Some of the *MCHI* genes in Atlantic cod carry signal peptides indicative of specialized use in cross-presentation of exogenous antigen (Malmstrom et al., 2013). Sub-functionalization of *MHCI* genes is further indicated by the different expression patterns observed for annotated *MHCI* in this study in combination with up-regulated *SEC61*, indicated to be crucial to the cross-presentation pathway (Gros and Amigorena, 2019). In contrast, we found no significant differential expression of the MHCI co-receptor *B2M* when looking at the qPCR results and investigating the raw counts (Supplementary Fig. 10).

3.5. Lymphocytes, antibodies and memory

In our experiment, there are some lymphocyte-related genes that are up-regulated, *CD40* and *CD83* for B-cells and *CD276* for T-cells. In addition, we observe the differential expression of a range of immunoglobulin chains, up-regulated on the two first time-points. However, the T-cell marker *CD8B* is actively down-regulated. This coincides with the up-regulation of *IL4I1* (Table 3), which in Atlantic cod most likely has antibacterial activity (Kitani et al., 2015), but has also been implied as a negative regulator of T-cell replication and activation in mammals (Boulland et al., 2007; Aubatin et al., 2018). Finally, we observe a few putative NK-like cell markers like *NCAM1* and *ITGAL*, but more specific markers like *LITR/NITR* (leukocyte immune-type receptors/novel immune-type receptors) and F-box protein 50 (non-specific cytotoxic cell receptor protein *NCCRP1*) are down-regulated. Thus, we observe a gene expression pattern indicating activation of B-cells only even though several of the up-regulated chemotactic cytokines are associated with T-cell and NK-like cell trafficking (Sokol and Luster, 2015).

The antibody response of an organism can be initiated with or

without T-cell help (Vinuesa and Chang, 2013). Since Atlantic cod lacks *CD4* (Star et al., 2011) there will be no conventional T-cell help, or help from other CD4+ cell lineages such as NKT-cells (Vinuesa and Chang, 2013). However, there are T-cell/NKT-cell help-independent mechanisms usually initiated through myeloid cells or directly with the B-cell itself if the antigen can provide a sufficiently strong signal upon interacting with the B-cell receptors (Vinuesa and Chang, 2013). In line with this, our transcriptome analysis reveals no up-regulation of genes involved in the conventional T-cell dependent or the more elaborate T-cell independent mechanisms. Thus, other systems such as direct B-cell stimulation with additional signals from surface TLRs or neutrophils is more likely (Vinuesa and Chang, 2013). Our data supports this by the up-regulation of *TLRs* and significant recruitment of neutrophils. It is also supported by the up-regulated *IL10* which can promote B-cell differentiation and IgM antibody secretion (Zou and Secombes, 2016).

3.6. Cell death as a defense mechanism

Cell death is a well-known defense mechanism for handling intracellular pathogens as well as a mechanism enabling proper clearance of immune cells, e.g. neutrophils whose content can result in tissue damage and the release of toxic compounds. It is dependent on detection through PRRs such as TLRs, NLRs and NK-cell receptors. Depending on the down-stream signaling pathway, the end result is either cell death (apoptosis) or pyroptosis (Schwartz et al., 2012; Storek and Monack, 2015). The former involves death receptors and caspases 2, 3, 7–10 (*CASP2, 3, 7–10*) leading to permeabilized cell membranes. Pyroptosis is dependent on the inflammasome and *CASP1, 4 and 5* and releases large amounts of pyrogens and inflammatory cytokines through lysis of host cells (Lai et al., 2015). Studies have found that various *Francisella* strains initiate both apoptosis and pyroptosis in mammalian cells. Our results demonstrate a stronger *CASP3* response and likely subsequent apoptosis supported by the pro-apoptopic genes *BAX*, *CASP6* and *CASP7*. *Francisella* strains have also been shown to inhibit the initiation of apoptosis in mammalian neutrophil cells where the natural onset of apoptosis begins within 12 h and is effective by 24 h. In our data, *CASP3* is seen at 6 h (Table 3) with additional caspases (*CASP 6 and 7*) appearing from day 2. This suggests a possible host-pathogen interaction in our experiment supported by earlier studies showing that *Francisella* infected neutrophils displayed onset of apoptosis after 48 h (Schwartz et al., 2012). Delaying apoptosis would facilitate pathogen survival, but also prolong the lifespan of immune cells. The latter would lead to dysregulation of the immune response facilitating e.g. the formation of granulomas in *Francisella* spp. infected organisms (Schwartz et al., 2012).

3.7. Summary and conclusion

In summary, we find that Atlantic cod, in response to *F. noatunensis*, transcribes genes classically associated with innate immunity related to pattern recognition, acute phase response and inflammation. However, in terms of adaptive immunity, we observe gene expression patterns that imply antigen presentation and cross-presentation by MHCI. Additionally, we uncover several contradictions in the expression of individual immune genes indicating that *F. noatunensis* modulates the Atlantic cod immune response. These findings are similar to other *Francisella* spp. infections described in mammals and fish with up-regulation of anti-inflammatory cytokines, down-regulated interferon gamma signaling, reduced ability to generate bactericidal phagosome environments and to produce reactive oxygen species, and delayed apoptosis. Furthermore, we observe down-regulation of T-cell markers and up-regulation of negative T-cell regulators. In contrast, there are several present B-cell markers and up-regulation of immunoglobulins suggesting a response involving direct stimulation of B-cells without the conventional help from T-cells or NKT-cells. In absence of conventional T/NKT-cell help, the strong presence of neutrophils markers in our data could provide support to the direct B-cell stimulation. However, based on the study conducted, we cannot completely determine if the observed results are due to the effects of the *F. noatunensis* infection and/or due to the alternative immune system of Atlantic cod. We also cannot observe any modulations on the level of translation with this particular kind of study. Any future experiments should extend beyond the sampled time-points to obtain a better picture of the adaptive response and contrast infections from both extracellular and intracellular pathogens to further unravel host-pathogen interactions from immune responses specific to Atlantic cod.

4. Methods

Please see GitHub repository for details: https://github.com/uio-cels/Solbakken_RNAseq

4.1. Fish and experiment setup

Parts of the overall challenge experiment have previously been published (without full transcriptome sequencing) (Seppola et al., 2016). Briefly, Atlantic cod juveniles (n = 66) from the Norwegian Atlantic cod breeding program (www.nofima.no) were transported at approx. 2 g to 100 l tanks at the Aquaculture Research Station (Tromsø, Norway) for grow-out in seawater of 3.4% salinity at 10 °C, 24 hour light and fed ad libitum with commercial feed (BioMar, Norway). The rates of water inflow were adjusted to an oxygen saturation of 90–100% in the outlet water. The fish were distributed in two circular, centrally drained, fiberglass tanks (250 l) with 30 fish in each tank (density < 20 kg/dm^3). The fish were reported to be healthy without any history of diseases. The experiment was approved by the National Animal Research authority in Norway (FOTS id 1147) and all methods were in accordance with the approved guidelines.

The *Francisella noatunensis* subsp. *noatunensis* NCIMB 14265 isolate used for challenge was originally isolated from diseased Atlantic cod (*Gadus morhua*) in Norway, and was provided by Dr. Duncan Colquhoun at the National Veterinary Institute Oslo, Norway (Mikalsen et al., 2007; strain described in Olsen et al., 2006). The bacteria were cultivated at 21 °C for 7–10 days on CHAB agar: heart infusion broth (Merck) pH 6.8 ± 0.2, supplemented with cysteine 0.1% (Merck, Germany), haemoglobin 2% (Oxoid, England), glucose 1%, agar 1.5% and 5% human blood concentrate. The bacteria were stored in glycerol cultures at −80 °C. Pure colonies were inoculated in Bacto heart infusion broth (Becton and Dickson, USA) pH 7, supplemented with cysteine 0.07%, $FeCl_3$ 2 mM and glucose 1%, and incubated with agitation at 21 °C for 24–30 h before being used in the challenge study. The bacterial cells were re-suspended to 0D at 600 nm 0.8, approximately 10^8 cfu/ml in 0.9% NaCl. CHAB plates were used for determination of colony forming units (cfu) of challenge dose and re-isolation of *F. noatunensis* from challenged fish. The cfu was determined to be 5 × 10^8 cfu/ml. To ensure the fish were infected with *F. noatunensis*, bacteria were re-isolated from infected fish. *F. noatunensis* were identified by colony appearance, white mucoid colonies, as well as by routine 16S rRNA analysis (data not shown).

The fish were acclimated to 15 °C and starved 24 h before injection. Prior to intra-peritoneal (ip) injection, the fish (approx. 25 g) were anaesthetised with Metacainum (50 mg/l, Norsk Medisinaldepot), and injected with 100 µl of either *F. noatunensis* (5×10^7 cfu per fish) or 0.9% NaCl (control). When sampled, fish were rapidly killed by cranial concussion and blood was removed by bleeding the fish from the *vena caudalis*. Head kidney and spleen from 6 individuals were sampled at 6 h, 1, 2, 4 and 7 days post challenge from both the treated and untreated groups (n = 60). Head kidney and spleen were aseptically removed and transferred to RNA-Later (Ambion) and kept at 4 °C overnight before being stored at −80 °C. No mortality was recorded in any of the tanks. Sample overview is presented in Supplementary Table 1.

4.2. RNA isolation and qPCR analyses

RNA was isolated from head kidney tissue as described earlier (Seppola et al., 2016) from all time-points. Briefly, tissues were homogenized in 1× lysis buffer using MagNA Lyser Green Beads and the MagNa Lyser Instrument (Roche Diagnostics). Total RNA was isolated using an ABI Prism 6100 Nucleic Acid Prep Station (Applied Biosystems) with the recommended on-column DNase treatment. Reverse transcription was performed using the High capacity RNA to cDNA master mix or High capacity cDNA reverse transcription kit (Applied Biosystems) with the addition of 2.5 mM poly dT primer (Promega). The reaction conditions were 25 °C (5–10 min), 42 °C (60–120 min) and 85 °C (5 min) and the cDNA was diluted 1:30 in nuclease free water (Ambion) for further use in quantitative real time PCR. Real time PCR was performed using the 7900HT Fast real-time PCR system and Power SYBR green PCR master mix according to the manufacturer's description (Applied Biosystems). Real time PCR primers have been published earlier (Seppola et al., 2008; Solstad et al., 2008; Furnes et al., 2009; Seppola et al., 2009; Bakkemo et al., 2011; Mikkelsen et al., 2011; Seppola et al., 2016) and are listed in Supplementary Table 2. Gene expression data were analyzed with the SDS 2.3 software (Applied Biosystems) and exported to Microsoft Excel for further analysis and plotted in R. The efficiency of the PCR reactions was determined by linear regression analysis of 2-fold dilutions of cDNA (total RNA isolated from cod head kidney) and denoted with a correlation coefficient (r2). Quantification of relative gene expression levels were performed using the $2-\Delta\Delta CT$ method57. For quantification of target genes expression among different organs, the geometric mean of 18S RNA was used for normalization. After normalization, the expression level was calibrated to uninfected controls. From relative quantification values obtained the mean quantity ± SEM was calculated. Statistical analyses between groups were made with the Student *t*-test and $p < 0.05$ was considered significant. qPCR results from hepcidin, cathelicidin and lysozyme are previously published (Bakkemo et al., 2011; Seppola et al., 2016)

4.3. RNA isolation, library preparation and RNA sequencing

Samples from 6 h, 2, 4 and 7 days post infection (and controls) were chosen for RNA sequencing (48 samples in total, see Supplementary Table 1). The samples and controls were subjected to the TRIzol reagent (Invitrogen) RNA isolation protocol. 30 mg of tissue was homogenized using sterile pistils in sterile 1.5 ml tubes (VWR) in 300 µl TRIzol reagent (Invitrogen). 60 µl of Chloroform (VWR International) and subsequently 150 µl of isopropanol (Sigma Aldrich) were added to the homogenate. Otherwise the TRIzol (Invitrogen) protocol was followed.

Some of the samples were taken from totalRNA to messengerRNA (mRNA) before library preparation (Supplementary Table 1). mRNA isolation was performed using the Dynabeads® mRNA direct kit (Life technologies) according to the manufacturers recommendations. This did not appear to affect sample clustering (Fig. 1). All RNA isolates (totalRNA or mRNA) were quality controlled using an Agilent 2100 Bioanalyzer (BioRad) before library preparation.

All libraries were prepared using the TruSeq™ RNA low-throughput (LT) protocol (Illumina). mRNA samples were included before the fragmentation step. All samples were fragmented for 4 min to obtain the size distribution desired according to the TruSeq protocol (library overview in Supplementary Table 1).

All libraries were sequenced 100 bp paired-end (PE) at the Norwegian Sequencing Centre on the Illumina HiSeq 2000 (www.sequencing.uio.no). Obtained sequences were cleaned for adapters using Cutadapt version 1.0 (Martin, 2012). Low quality regions were trimmed using Sickle with a 40 bp minimum remaining sequence length, a Sanger quality threshold of 20 and no 5′ end trimming (Joshi, n.d.). Results were quality controlled using FastQC version 0.9.2 to ensure improvement compared to raw data (Andrews, 2011). Data is available from ENA: PRJEB31396.

4.4. Methodological considerations for large scale RNAseq analysis on a non-model species

The Atlantic cod genome was first published in 2011 (Star et al., 2011) and consisted on only 454 sequencing using both shotgun and paired-end libraries to an average coverage of 40×. In 2017 Tørresen et al. released an improved version of the cod genome (gadMor2) adding BAC-ends, Illumina and PacBio sequencing data to improve genome resolution. The genome is a reconciled assembly where the best features of 4 subassemblies were combined. Furthermore, it also contains an unusual amount of tandem repeats (Torresen et al., 2017). Our observation is that immune-related genes often are located to genomic regions with repeats or poor resolution and often without annotation. Thus, we opted to analyze the RNAseq data using both a reference-based (TopHat/Cufflinks) and a de novo (Trinity) strategy to better capture unassembled, partially or un-annotated (immune) genes providing the best possible resolution of the genetic background in Atlantic cod before performing differential expression analysis.

In terms of differential expression, the data have been analyzed in a pairwise manner, with a general linearized model (GLM) time:-treatment as well as a custom script clustering genes according to five given expression profiles in a control-dependent manner. Details are given below.

4.5. Reference-genome based approach using Tuxedo

The second version of the Atlantic cod genome (Torresen et al., 2017) was used as the genomic reference for a Tophat/Cufflinks pipeline according to the workflow described in Trapnell et al. (2012). Mapping of samples towards the reference-genome GFF3 file was performed with Tophat v2.0.14 with default settings. Sample-specific transcriptomes were generated with Cufflinks v2.1.1. Cuffmerge was used to concatenate all the individual transcriptomes. Differential expression analysis was performed with Cuffdiff in a pairwise manner between treated and control for each time-point. The output from Cuffdiff was further explored using CummeRbund v2.8.2 in R v3.1.3 for presentation purposes (Goff et al., 2013; R-Core-Team, 2015). An overview of the analysis is presented in the supplementary information (SFigs. 6 and 7). Significantly differentially expressed genes are listed in Supplementary excel file 1. Read counts were also extracted from the Cuffdiff experiment and analyzed using the custom script as described below. Significant genes from this analysis are listed in Supplementary excel file 2.

4.6. Reference-genome-guided approach using Trinity

Two RNAseq studies provided reads for the transcriptome assembly used here – the reads derived from the *Francisella* challenge described above and the reads derived from a vibriosis vaccination study with the same number of samples (vaccination study has previously been reported and samples are derived from the vibriosis susceptible family which establishes good protection post vaccination (Mikkelsen and Seppola, 2013), RNAseq study Solbakken et al., Under Review). In total, the 96 libraries (48 from each experiment) provided on average 20.51 million trimmed read-pairs resulting in 1969.31 million reads in total.

We applied the Trinity transcriptome assembler v 2.0.6 using the genome-guided option with the second version of the Atlantic cod genome (Torresen et al., 2017).The genome was indexed using Bowtie1 (v1.0.0) and then mapped using Tophat (v2.0.9) and sorted with Samtools (v0.1.19). The built-in normalization step of Trinity was applied reducing the trimmed read dataset to approximately 45 million read pairs (Grabherr et al., 2011; Haas et al., 2013). The following parameters were changed for the Trinity run: genome-guided, max intron 10,000, max memory 150 Gb, bflyHeapSpaceMax 10G, bflyCPU 12

and CPU 10.

The assembly was evaluated with the built-in trinity_stats.pl and align_and_estimate_abundance.pl — the latter with RSEM estimation method and bowtie aligner. The abundance estimation output was further used to filter the assembly on transcript level with FPKM = 1 using filter_fasta_by_rsem_values.pl. This resulted in 44,543 transcripts with an overall contig N50 of 2568 bp, median contig length of 1132 bp and a total of ~73.3 million assembled bases. Based on the longest open reading frames (ORFs) the transcript dataset was reduced to 32,934 "genes" with an overall contig N50 of 2490 bp and median contig length of 1014 bp.

Overall annotation was performed using Trinotate v. 2.0.1 following all mandatory steps with default parameters on the non-filtered assembly and transferred to the filtered assembly transcripts. The annotation of genes specifically discussed in this study have been verified through reciprocal BLAST by extracting the longest isoform of the gene in question and subjecting it to a BLASTX towards all UniProt entries using the UniProt BLAST tool with default settings (UniProt, 2015).

In addition, a list of specific immune genes was annotated manually (Supplementary Table 3). Queries from human and at least 3 fish species was downloaded from UniProt and/or Genbank and aligned in MEGA7 (Kumar et al., 2016) to ensure sequence homology. The queries were used in a TBLASTN (Camacho et al., 2009) search towards the Trinity assembly using tabular output, default parameters and an e-value cutoff of 1e-1. All transcript hits were extracted and the longest isoform selected for a reciprocal BLASTX using the NCBI online BLAST tool. When needed, the extracted isoform was also aligned towards the queries in MEGA7 to evaluate hit accuracy. A list of conservatively annotated transcripts is presented in Supplementary Table 3.

4.7. Sample mapping, read count extraction

The trimmed reads from all Francisella-related samples were mapped against the filtered Trinity assembly using the built-in align_and_estimate_abundance script in Trinity with RSEM estimation method and bowtie aligner, before extracting raw counts using abundance_estimates_to_matrix.pl again with RSEM as the estimation method. For the Trinity-generated read-counts, the variance within the experiment was explored using the R-package VariancePartition (Hoffman and Schadt, 2016). Differential expression analysis was first analyzed in a pairwise manner using an edgeR script included in the Trinity program. Then, the same counts were subjected to a GLM-based analysis time:treatment using glmQLFit and glmQLFTest. Finally, the read counts were analyzed using the custom script as described below. An overview of the analysis is presented in SFigs. 1–5). All significantly differentially expressed genes are reported in Supplementary excel file 3 (default pairwise analysis), Supplementary excel file 4 (time:-treatment GLM) and Supplementary excel file 5 (custom script).

4.8. Error distributions

Most RNAseq analysis packages assume that such data follows a negative binomial distribution of variability. We tested this assumption using a custom script testing the fit of the Poisson distribution, the negative binomial distribution and the zero-inflated negative binomial distribution (using the pscl package in R, script available in the GitHub repository). About 90% of all genes were classified as having negative binomial distribution and thus, in all cases, the negative binomial distribution was used for all down-stream analyses (data not shown, available in Github repository).

4.9. Custom script approach for gene expression pattern clustering

We wanted to further characterize the behavior of the dataset outside of what the most common "clustering by expression" RNAseq analysis packages could provide. In this way we could take into account our continuous control samples (contrary to only having a single time 0 control group) and define the expression patterns beforehand. This categorization was performed with a set of GLM regression models; no time dependency, linear time dependency, quadratic time dependency, factorial time dependency, pure treatment effect (no time dependency), treatment combined with linear time (interaction), treatment combined with quadratic time (interaction) and treatment combined with factorial time (interaction). Estimated regression coefficients were then used to determine in which category each gene's expression was to be assigned using the conservative BIC model selection criterion. In this manuscript the expression profiles are described as 'increasing over time', 'internal maximum', 'decrease over time', 'internal minimum' and 'freestyle'. Only data from the control-dependent analyses are shown. (Note that if a quadratic effect was found but with minima/maxima outside the data material, it would be classified as either increasing or decreasing, depending on the estimated quadratic effect).

4.10. GO and gene network analyses

For all significant differentially expressed genes the (if available) corresponding annotation was translated to the "human" gene name in cases of clear orthology. In cases where orthology was questionable the automated annotation remained. In the de novo transcriptome assembly several genes had obtained multiple annotations. Here, the longest isoform was manually subjected to a BLASTX at the NCBI BLAST server with default settings and restricting the database to teleostei only. The multi-annotation was converted to a single annotation whenever possible. All significantly differentially expressed genes with corresponding annotation reported from all analyses above were analyzed in Cytoscape (Shannon et al., 2003) using the plugin ClueGO (Bindea et al., 2009). ClueGO performs a GO term enrichment (two-sided hypergeometric test for both enrichment and depletion) and was run selecting a full GO term analysis with otherwise default parameters. The Bonferroni step-down p-value cutoff was set to p = o.o5 unless otherwise stated. GO term fusion (related terms that share similar genes are fused) was applied to the larger networks to improve readability (specifically stated). In some cases, a GO term analysis specifying only immune-related GO terms was run (specifically stated). The layout of the networks was manually rearranged to improve readability. Size of the nodes corresponds to the corrected p-value. The thickness of the edges (lines) connecting the nodes represents the kappa score – the degree of connectivity between two nodes based on their overlapping genes.

Conflict of interest

All authors have read and approved the manuscript. We declare no conflicts of interest. We also declare that all handling of animals was done according to regulations in Norway and that the experiment has been approved by local animal welfare authorities.

Acknowledgements

This work was supported by Research Council of Norway (Grant numbers 199806/S40 and 222378/F20 to KSJ/SJ and grant number 199672/E40 to MS). The reference-genome assembly was made using the Abel Cluster, owned by the University of Oslo and the Norwegian metacenter for High Performance Computing (NOTUR), and operated by the Department for Research Computing at USIT, the University of Oslo IT-department. http://www.hpc.uio.no/. The sequencing service was provided by the Norwegian Sequencing Centre (www.sequencing.uio.no), a national technology platform hosted by the University of Oslo.

Additional information

This manuscript has a GitHub repository providing all data: https://github.com/uio-cels/Solbakken_RNAseq. Sequencing data is available through ENA: PRJEB31396 (additional sequences included in the transcriptome PRJEB31369).

Competing financial interests

The authors declare no competing financial interests.

Appendix A. Supplementary data

Supplementary data to this article can be found online at https://doi.org/10.1016/j.cbd.2019.04.004.

References

Andrews, S., 2011. The FastQC project. http://www.bioinformatics.babraham.ac.uk/projects/fastqc/.

Asare, R., Kwaik, Y.A., 2010. Exploitation of host cell biology and evasion of immunity by francisella tularensis. Front. Microbiol. 1, 145.

Aubatin, A., Sako, N., Decrouy, X., Donnadieu, E., Molinier-Frenkel, V., Castellano, F., 2018. IL4-induced gene 1 is secreted at the immune synapse and modulates TCR activation independently of its enzymatic activity. Eur. J. Immunol. 48, 106–119.

Bakkemo, K.R., Mikkelsen, H., Bordevik, M., Torgersen, J., Winther-Larsen, H.C., Vanberg, C., Olsen, R., Johansen, L.H., Seppola, M., 2011. Intracellular localisation and innate immune responses following Francisella noatunensis infection of Atlantic cod (Gadus morhua) macrophages. Fish Shellfish Immunol 31, 993–1004.

Bakkemo, K.R., Mikkelsen, H., Johansen, A., Robertsen, B., Seppola, M., 2016. Francisella noatunensis subsp. noatunensis invades, survives and replicates in Atlantic cod cells. Dis. Aquat. Org. 121, 149–159.

Bindea, G., Mlecnik, B., Hackl, H., Charoentong, P., Tosolini, M., Kirilovsky, A., Fridman, W.H., Pages, F., Trajanoski, Z., Galon, J., 2009. ClueGO: a Cytoscape plug-in to decipher functionally grouped gene ontology and pathway annotation networks. Bioinformatics (Oxford, England) 25, 1091–1093.

Birkbeck, T.H., Feist, S.W., Verner-Jeffreys, D.W., 2011. Francisella infections in fish and shellfish. J. Fish Dis. 34, 173–187.

Bottazzi, B., Inforzato, A., Messa, M., Barbagallo, M., Magrini, E., Garlanda, C., Mantovani, A., 2016. The pentraxins PTX3 and SAP in innate immunity, regulation of inflammation and tissue remodelling. J. Hepatol. 64, 1416–1427.

Boulland, M.L., Marquet, J., Molinier-Frenkel, V., Moller, P., Guiter, C., Lasoudris, F., Copie-Bergman, C., Baia, M., Gaulard, P., Leroy, K., Castellano, F., 2007. Human IL4I1 is a secreted L-phenylalanine oxidase expressed by mature dendritic cells that inhibits T-lymphocyte proliferation. Blood 110, 220–227.

Brubaker, S.W., Bonham, K.S., Zanoni, I., Kagan, J.C., 2015. Innate immune pattern recognition: a cell biological perspective. Annu. Rev. Immunol. 33, 257–290.

Brudal, E., Ulanova, L.S., E, O.L., Rishovd, A.L., Griffiths, G., Winther-Larsen, H.C., 2014. Establishment of three Francisella infections in zebrafish embryos at different temperatures. Infect. Immun. 82, 2180–2194.

Camacho, C., Coulouris, G., Avagyan, V., Ma, N., Papadopoulos, J., Bealer, K., Madden, T.L., 2009. BLAST+: architecture and applications. BMC bioinformatics 10, 421.

Colquhoun, D.J., Duodu, S., 2011. Francisella infections in farmed and wild aquatic organisms. Vet. Res. 42, 47.

Drickamer, K., Taylor, M.E., 2015. Recent insights into structures and functions of C-type lectins in the immune system. Curr. Opin. Struct. Biol. 34, 26–34.

Ellingsen, T., Inami, M., Gjessing, M.C., Van Nieuwenhove, K., Larsen, R., Seppola, M., Lund, V., Schroder, M.B., 2011. Francisella noatunensis in Atlantic cod (Gadus morhua L.); waterborne transmission and immune responses. Fish Shellfish Immunol 31, 326–333.

Flajnik, M.F., 2018. A cold-blooded view of adaptive immunity. Nat. Rev. Immunol. 18, 438–453.

Furevik, A., Pettersen, E.F., Colquhoun, D., Wergeland, H.I., 2011. The intracellular lifestyle of Francisella noatunensis in Atlantic cod (Gadus morhua L.) leucocytes. Fish Shellfish Immunol 30, 488–494.

Furnes, C., Seppola, M., Robertsen, B., 2009. Molecular characterisation and expression analysis of interferon gamma in Atlantic cod (Gadus morhua). Fish Shellfish Immunol 26, 285–292.

Gjessing, M.C., Inami, M., Weli, S.C., Ellingsen, T., Falk, K., Koppang, E.O., Kvellestad, A., 2011. Presence and interaction of inflammatory cells in the spleen of Atlantic cod, Gadus morhua L., infected with Francisella noatunensis. J. Fish Dis. 34, 687–699.

Goff, L., Trapnell, C., Kelley, D., 2013. cummeRbund: Analysis, exploration, manipulation, and visualization of Cufflinks high-throughput sequencing ata, R package version 2.8.2 ed. http://bioconductor.org/packages/release/bioc/html/cummeRbund.html.

Grabherr, M.G., Haas, B.J., Yassour, M., Levin, J.Z., Thompson, D.A., Amit, I., Adiconis, X., Fan, L., Raychowdhury, R., Zeng, Q., Chen, Z., Mauceli, E., Hacohen, N., Gnirke, A., Rhind, N., di Palma, F., Birren, B.W., Nusbaum, C., Lindblad-Toh, K., Friedman, N., Regev, A., 2011. Full-length transcriptome assembly from RNA-Seq data without a reference genome. Nat. Biotechnol. 29, 644–652.

Grimholt, U., 2016. MHC and Evolution in Teleosts. Biology 5.

Gros, M., Amigorena, S., 2019. Regulation of Antigen Export to the Cytosol During Cross-Presentation. Front. Immunol. 10, 41.

Haas, B.J., Papanicolaou, A., Yassour, M., Grabherr, M., Blood, P.D., Bowden, J., Couger, M.B., Eccles, D., Li, B., Lieber, M., MacManes, M.D., Ott, M., Orvis, J., Pochet, N., Strozzi, F., Weeks, N., Westerman, R., William, T., Dewey, C.N., Henschel, R., LeDuc, R.D., Friedman, N., Regev, A., 2013. De novo transcript sequence reconstruction from RNA-seq using the Trinity platform for reference generation and analysis. Nat. Protoc. 8, 1494–1512.

Havixbeck, J.J., Barreda, D.R., 2015. Neutrophil Development, Migration, and Function in Teleost Fish. Biology 4, 715–734.

Hoffman, G.E., Schadt, E.E., 2016. variancePartition: interpreting drivers of variation in complex gene expression studies. BMC bioinformatics 17, 483.

Howe, K., Schiffer, P.H., Zielinski, J., Wiehe, T., Laird, G.K., Marioni, J.C., Soylemez, O., Kondrashov, F., Leptin, M., 2016. Structure and evolutionary history of a large family of NLR proteins in the zebrafish. Open Biol. 6, 160009.

Isachsen, C.H., Vagnes, O., Jakobsen, R.A., Samuelsen, O.B., 2012. Antimicrobial susceptibility of Francisella noatunensis subsp. noatunensis strains isolated from Atlantic cod Gadus morhua in Norway. Dis. Aquat. Org. 98, 57–62.

Jones, C.L., Napier, B.A., Sampson, T.R., Llewellyn, A.C., Schroeder, M.R., Weiss, D.S., 2012. Subversion of host recognition and defense systems by Francisella spp. Microbiology and molecular biology reviews : MMBR 76, 383–404.

Joshi, N. Sickle - a windowed adaptive trimming tool for FASTQ files using quality. https://github.com/ucdavis-bioinformatics/sickle.

Kawasaki, T., Kawai, T., 2014. Toll-like receptor signaling pathways. Front. Immunol. 5, 461.

Kitani, Y., Fernandes, J.M., Kiron, V., 2015. Identification of the Atlantic cod L-amino acid oxidase and its alterations following bacterial exposure. Dev. Comp. Immunol. 50, 116–120.

Klebanoff, S.J., Kettle, A.J., Rosen, H., Winterbourn, C.C., Nauseef, W.M., 2013. Myeloperoxidase: a front-line defender against phagocytosed microorganisms. J. Leukoc. Biol. 93, 185–198.

Klinger-Bowen, R., Tamaru, C., McGovern-Hopkins, K., Li, Y., Sithole, F., Kearney, M.T., Francis, S., Soto, E., 2016. Dynamics of piscine francisellosis differs amongst tilapia species (Oreochromis spp.) in a controlled challenge with Francisella noatunensis subsp. orientalis. J. Fish Dis. 39, 1305–1312.

Kufer, T.A., Sansonetti, P.J., 2011. NLR functions beyond pathogen recognition. Nat. Immunol. 12, 121–128.

Kumar, S., Stecher, G., Tamura, K., 2016. MEGA7: Molecular Evolutionary Genetics Analysis Version 7.0 for Bigger Datasets. Mol. Biol. Evol. 33, 1870–1874.

Kuri, P., Schieber, N.L., Thumberger, T., Wittbrodt, J., Schwab, Y., Leptin, M., 2017. Dynamics of in vivo ASC speck formation. J. Cell Biol. 216, 2891–2909.

Lagos, L., Tandberg, J.I., Repnik, U., Boysen, P., Ropstad, E., Varkey, D., Paulsen, I.T., Winther-Larsen, H.C., 2017. Characterization and Vaccine Potential of Membrane Vesicles Produced by Francisella noatunensis subsp. orientalis in an Adult Zebrafish Model. Clin. Vaccine Immunol. 24.

Lai, X.H., Xu, Y., Chen, X.M., Ren, Y., 2015. Macrophage cell death upon intracellular bacterial infection. Macrophage 2, e779.

Leal, C.A., Tavares, G.C., Figueiredo, H.C., 2014. Outbreaks and genetic diversity of Francisella noatunensis subsp orientalis isolated from farm-raised Nile tilapia (Oreochromis niloticus) in Brazil. Genetics and molecular research : GMR 13, 5704–5712.

Li, J.Y., Gao, K., Shao, T., Fan, D.D., Hu, C.B., Sun, C.C., Dong, W.R., Lin, A.F., Xiang, L.X., Shao, J.Z., 2018. Characterization of an NLRP1 Inflammasome from Zebrafish Reveals a Unique Sequential Activation Mechanism Underlying Inflammatory Caspases in Ancient Vertebrates. J. Immunol. 201 (7), 1946–1966. https://doi.org/10.4049/jimmunol.1800498.

Li, Y., Huang, Y., Cao, X., Yin, X., Jin, X., Liu, S., Jiang, J., Jiang, W., Xiao, T.S., Zhou, R., Cai, G., Hu, B., Jin, T., 2018. Functional and structural characterization of zebrafish ASC. FEBS J. 285, 2691–2707.

Maekawa, S., Wang, P.C., Chen, S.C., 2019. Comparative Study of Immune Reaction Against Bacterial Infection From Transcriptome Analysis. Front. Immunol. 10, 153.

Malmstrom, M., Jentoft, S., Gregers, T.F., Jakobsen, K.S., 2013. Unraveling the evolution of the Atlantic cod's (Gadus morhua L.) alternative immune strategy. PLoS One 8, e74004.

Malmstrom, M., Matschiner, M., Torresen, O.K., Star, B., Snipen, L.G., Hansen, T.F., Baalsrud, H.T., Nederbragt, A.J., Hanel, R., Salzburger, W., Stenseth, N.C., Jakobsen, K.S., Jentoft, S., 2016. Evolution of the immune system influences speciation rates in teleost fishes. Nat. Genet. 48, 1204–1210.

Martin, M., 2012. Cutadapt removes adapter sequences from high-throughput sequencing reads. Bioinformatics in Action 17, 10–12.

McCaffrey, R.L., Allen, L.A., 2006. Francisella tularensis LVS evades killing by human neutrophils via inhibition of the respiratory burst and phagosome escape. J. Leukoc. Biol. 80, 1224–1230.

McCaffrey, R.L., Schwartz, J.T., Lindemann, S.R., Moreland, J.G., Buchan, B.W., Jones, B.D., Allen, L.A., 2010. Multiple mechanisms of NADPH oxidase inhibition by type A and type B Francisella tularensis. J. Leukoc. Biol. 88, 791–805.

Mikalsen, J., Olsen, A.B., Tengs, T., Colquhoun, D.J., 2007. Francisella philomiragia subsp. noatunensis subsp. nov., isolated from farmed Atlantic cod (Gadus morhua L.). Int. J. Syst. Evol. Microbiol. 57, 1960–1965.

Mikkelsen, H., Lund, V., Larsen, R., Seppola, M., 2011. Vibriosis vaccines based on various sero-subgroups of Vibrio anguillarum O2 induce specific protection in Atlantic cod (Gadus morhua L.) juveniles. Fish Shellfish Immunol 30, 330–339.

Mikkelsen, H., Seppola, M., 2013. Response to vaccination of Atlantic cod (Gadus morhua L.) progenies from families with different estimated family breeding values for vibriosis resistance. Fish Shellfish Immunol 34, 387–392.

Nairz, M., Dichtl, S., Schroll, A., Haschka, D., Tymoszuk, P., Theurl, I., Weiss, G., 2018. Iron and innate antimicrobial immunity-Depriving the pathogen, defending the host. Journal of trace elements in medicine and biology : organ of the Society for Minerals and Trace Elements (GMS) 48, 118–133.
Olsen, A.B., Mikalsen, J., Rode, M., Alfjorden, A., Hoel, E., Straum-Lie, K., Haldorsen, R., Colquhoun, D.J., 2006. A novel systemic granulomatous inflammatory disease in farmed Atlantic cod, Gadus morhua L., associated with a bacterium belonging to the genus Francisella. J. Fish Dis. 29, 307–311.
Pauwels, A.M., Trost, M., Beyaert, R., Hoffmann, E., 2017. Patterns, Receptors, and Signals: Regulation of Phagosome Maturation. Trends Immunol. 38, 407–422.
R-Core-Team, 2015. R: A Language and Environment for Statistical Computing. https://www.r-project.org/.
Riera Romo, M., Perez-Martinez, D., Castillo Ferrer, C., 2016. Innate immunity in vertebrates: an overview. Immunology 148, 125–139.
Schrøder, M.B., Ellingsen, T., Mikkelsen, H., Norderhus, E.A., Lund, V., 2009. Comparison of antibody responses in Atlantic cod (Gadus morhua L.) to Vibrio anguillarum, Aeromonas salmonicida and Francisella sp. Fish Shellfish Immunol 27, 112–119.
Schwartz, J.T., Barker, J.H., Kaufman, J., Fayram, D.C., McCracken, J.M., Allen, L.A., 2012. Francisella tularensis inhibits the intrinsic and extrinsic pathways to delay constitutive apoptosis and prolong human neutrophil lifespan. J. Immunol. 188, 3351–3363.
Secombes, C.J., 2016. What's new in fish cytokine research? Fish Shellfish Immunol 53, 1–3.
Seppola, M., Bakkemo, K.R., Mikkelsen, H., Myrnes, B., Helland, R., Irwin, D.M., Nilsen, I.W., 2016. Multiple specialised goose-type lysozymes potentially compensate for an exceptional lack of chicken-type lysozymes in Atlantic cod. Sci. Rep. 6, 28318.
Seppola, M., Johnsen, H., Mennen, S., Myrnes, B., Tveiten, H., 2009. Maternal transfer and transcriptional onset of immune genes during ontogenesis in Atlantic cod. Dev. Comp. Immunol. 33, 1205–1211.
Seppola, M., Larsen, A.N., Steiro, K., Robertsen, B., Jensen, I., 2008. Characterisation and expression analysis of the interleukin genes, IL-1beta, IL-8 and IL-10, in Atlantic cod (Gadus morhua L.). Mol. Immunol. 45, 887–897.
Shannon, P., Markiel, A., Ozier, O., Baliga, N.S., Wang, J.T., Ramage, D., Amin, N., Schwikowski, B., Ideker, T., 2003. Cytoscape: a software environment for integrated models of biomolecular interaction networks. Genome Res. 13, 2498–2504.
Sokol, C.L., Luster, A.D., 2015. The chemokine system in innate immunity. Cold Spring Harb. Perspect. Biol. 7.
Solbakken, M.H., Rise, M.L., Jakobsen, K.S., Jentoft, S., 2016. Successive Losses of Central Immune Genes Characterize the Gadiformes' Alternate Immunity. Genome biology and evolution 8, 3508–3515.
Solbakken, M.H., Torresen, O.K., Nederbragt, A.J., Seppola, M., Gregers, T.F., Jakobsen, K.S., Jentoft, S., 2016. Evolutionary redesign of the Atlantic cod (Gadus morhua L.) Toll-like receptor repertoire by gene losses and expansions. Sci. Rep. 6, 25211.
Solbakken, M.H., Voje, K.L., Jakobsen, K.S., Jentoft, S., 2017. Linking species habitat and past palaeoclimatic events to evolution of the teleost innate immune system. Proc. Biol. Sci. 284.
Solstad, T., Larsen, A.N., Seppola, M., Jorgensen, T.O., 2008. Identification, cloning and expression analysis of a hepcidin cDNA of the Atlantic cod (Gadus morhua L.). Fish Shellfish Immunol 25, 298–310.
Soto, E., Kidd, S., Gaunt, P.S., Endris, R., 2013. Efficacy of florfenicol for control of mortality associated with Francisella noatunensis subsp. orientalis in Nile tilapia, Oreochromis niloticus (L.). J. Fish Dis. 36, 411–418.
Soto, E., McGovern-Hopkins, K., Klinger-Bowen, R., Fox, B.K., Brock, J., Antonio, N., Waal, Z., Rushton, S., Mill, A., Tamaru, C.S., 2013. Prevalence of Francisella noatunensis subsp. orientalis in cultured tilapia on the island of Oahu, Hawaii. J. Aquat. Anim. Health 25, 104–109.
Soto, E., Primus, A.E., Pouder, D.B., George, R.H., Gerlach, T.J., Cassle, S.E., Johnson, T., Boyd, S., Handsel, T., Yanong, R.P., 2014. Identification of Francisella noatunensis in novel host species French grunt (Haemulon flavolineatum) and Caesar grunt (Haemulon carbonarium). Journal of zoo and wildlife medicine : official publication of the American Association of Zoo Veterinarians 45, 727–731.
Star, B., Nederbragt, A.J., Jentoft, S., Grimholt, U., Malmstrom, M., Gregers, T.F., Rounge, T.B., Paulsen, J., Solbakken, M.H., Sharma, A., Wetten, O.F., Lanzen, A., Winer, R., Knight, J., Vogel, J.H., Aken, B., Andersen, O., Lagesen, K., Tooming-Klunderud, A., Edvardsen, R.B., Tina, K.G., Espelund, M., Nepal, C., Previti, C., Karlsen, B.O., Moum, T., Skage, M., Berg, P.R., Gjoen, T., Kuhl, H., Thorsen, J., Malde, K., Reinhardt, R., Du, L., Johansen, S.D., Searle, S., Lien, S., Nilsen, F., Jonassen, I., Omholt, S.W., Stenseth, N.C., Jakobsen, K.S., 2011. The genome sequence of Atlantic cod reveals a unique immune system. Nature 477, 207–210.
Steiner, D.J., Furuya, Y., Metzger, D.W., 2014. Host-pathogen interactions and immune evasion strategies in Francisella tularensis pathogenicity. Infection and drug resistance 7, 239–251.
Storek, K.M., Monack, D.M., 2015. Bacterial recognition pathways that lead to inflammasome activation. Immunol. Rev. 265, 112–129.
Sundaram, A.Y., Kiron, V., Dopazo, J., Fernandes, J.M., 2012. Diversification of the expanded teleost-specific toll-like receptor family in Atlantic cod, Gadus morhua. BMC Evol. Biol. 12, 256.
Szabady, R.L., McCormick, B.A., 2013. Control of neutrophil inflammation at mucosal surfaces by secreted epithelial products. Front. Immunol. 4, 220.
Torresen, O.K., Brieuc, M.S.O., Solbakken, M.H., Sorhus, E., Nederbragt, A.J., Jakobsen, K.S., Meier, S., Edvardsen, R.B., Jentoft, S., 2018. Genomic architecture of haddock (Melanogrammus aeglefinus) shows expansions of innate immune genes and short tandem repeats. BMC Genomics 19, 240.
Torresen, O.K., Star, B., Jentoft, S., Reinar, W.B., Grove, H., Miller, J.R., Walenz, B.P., Knight, J., Ekholm, J.M., Peluso, P., Edvardsen, R.B., Tooming-Klunderud, A., Skage, M., Lien, S., Jakobsen, K.S., Nederbragt, A.J., 2017. An improved genome assembly uncovers prolific tandem repeats in Atlantic cod. BMC Genomics 18, 95.
Trapnell, C., Roberts, A., Goff, L., Pertea, G., Kim, D., Kelley, D.R., Pimentel, H., Salzberg, S.L., Rinn, J.L., Pachter, L., 2012. Differential gene and transcript expression analysis of RNA-seq experiments with TopHat and Cufflinks. Nat. Protoc. 7, 562–578.
Ulanova, L.S., Pinheiro, M., Vibe, C., Nunes, C., Misaghian, D., Wilson, S., Zhu, K., Fenaroli, F., Winther-Larsen, H.C., Reis, S., Griffiths, G., 2017. Treatment of Francisella infections via PLGA- and lipid-based nanoparticle delivery of antibiotics in a zebrafish model. Dis. Aquat. Org. 125, 19–29.
UniProt, C., 2015. UniProt: a hub for protein information. Nucleic Acids Res. 43, D204–D212.
Vestvik, N., Ronneseth, A., Kalgraff, C.A., Winther-Larsen, H.C., Wergeland, H.I., Haugland, G.T., 2013. Francisella noatunensis subsp. noatunensis replicates within Atlantic cod (Gadus morhua L.) leucocytes and inhibits respiratory burst activity. Fish Shellfish Immunol 35, 725–733.
Vinuesa, C.G., Chang, P.P., 2013. Innate B cell helpers reveal novel types of antibody responses. Nat. Immunol. 14, 119–126.
Vojtech, L.N., Sanders, G.E., Conway, C., Ostland, V., Hansen, J.D., 2009. Host immune response and acute disease in a zebrafish model of Francisella pathogenesis. Infect. Immun. 77, 914–925.
Wang, T., Secombes, C.J., 2013. The cytokine networks of adaptive immunity in fish. Fish Shellfish Immunol 35, 1703–1718.
Wcisel, D.J., Yoder, J.A., 2016. The confounding complexity of innate immune receptors within and between teleost species. Fish Shellfish Immunol 53, 24–34.
Wiegertjes, G.F., Wentzel, A.S., Spaink, H.P., Elks, P.M., Fink, I.R., 2016. Polarization of immune responses in fish: The 'macrophages first' point of view. Mol. Immunol. 69, 146–156.
Wilson, A.B., 2017. MHC and adaptive immunity in teleost fishes. Immunogenetics 69, 521–528.
Zhu, L.Y., Nie, L., Zhu, G., Xiang, L.X., Shao, J.Z., 2013. Advances in research of fish immune-relevant genes: a comparative overview of innate and adaptive immunity in teleosts. Dev. Comp. Immunol. 39, 39–62.
Zou, J., Secombes, C.J., 2011. Teleost fish interferons and their role in immunity. Dev. Comp. Immunol. 35, 1376–1387.
Zou, J., Secombes, C.J., 2016. The Function of Fish Cytokines. Biology 5.